Imaging in oral cancers

Supreeta Arya, Devendra Chaukar[1], Prathamesh Pai[1]

Departments of Radio-diagnosis, and [1]Surgical Oncology, Tata Memorial Hospital, Mumbai, Maharashtra, India

Correspondence: Dr. Supreeta Arya, Department of Radiodiagnosis, Tata Memorial Hospital, Parel, Mumbai - 400 012, India.
E-mail: supreeta.arya@gmail.com

Abstract

Oral cavity squamous cell cancers form a significant percentage of the cancers seen in India. While clinical examination allows direct visualization, it cannot evaluate deep extension of disease. Cross-sectional imaging has become the cornerstone in the pretreatment evaluation of these cancers and provides accurate information about the extent and depth of disease that can help decide the appropriate management strategy and indicate prognosis. Early cancers are treated with a single modality, either surgery or radiotherapy while advanced cancers are offered a combination of surgery, radiotherapy and chemotherapy. Imaging can decide resectability, help plan the precise extent of resection, and indicate whether organ conservation therapy should be offered. Quality of life issues necessitate preservation of form and function and pretreatment imaging helps plan appropriate reconstruction and counsel patients regarding lifestyle changes. Oral cavity has several subsites and the focus of the review is squamous cancers of the gingivobuccal region, oral tongue and retromolar trigone as these are most frequently encountered in the subcontinent. References for this review were identified by searching Medline and PubMed databases. Only articles published in English language literature were selected. This review aims to familiarize the radiologist with the relevant anatomy of the oral cavity, discuss the specific issues that influence prognosis and management at the above subsites, the optimal imaging methods, the role of imaging in accurately staging these cancers and in influencing management. A checklist for reporting will emphasize the information to be conveyed by the radiologist.

Key words: CT; cancers, gingivobuccal; imaging, MRI; tongue

Introduction

Oral cancers form nearly 30% of the cancers presenting at our tertiary referral institute, the age adjusted incidence in India being 20 per 100,000 population.[1] Squamous cell cancers (SCC) form the bulk (more than 90%) with tobacco chewing and alcohol being the dominant causes. Imaging provides crucial information for appropriate management of these cancers. Awareness of specific issues related to spread of oral cancers at various subsites and the principles of management would help the radiologist choose an optimal method of imaging and provide the clinician with a relevant report. In this article we will focus on SCC of the gingivobuccal complex and oral tongue.

Methods

References for this review were identified by searching Medline and PubMed databases. Only articles published in English language literature were used. The search terms used were CT oral squamous cancers, CT MRI buccal cancers, mandibular invasion oral cancers, gingivobuccal cancer, retromolar trigone, imaging neck node metastases, neck node dissection, MRI tongue, MRI tongue tumor thickness, and diffusion-weighted imaging neck nodes. Cross references from relevant articles were also included. This review is evidence based, but also reflects our experience in the management of oral cancers at the largest tertiary referral cancer center in India.

Anatomy of the Oral Cavity

The oral cavity extends from the lips to a circular region behind, comprising of the circumvallate papillae on the tongue dorsum, anterior tonsillar pillars on either side, reaching upto the junction of hard palate and soft palate superiorly. The papillae are not identified on imaging.

The oral cavity is divided into a central part "the oral cavity proper" and a lateral part "the vestibule" [Figure 1]. The oral cavity proper consists of the central tongue, the roof formed by the hard palate, the lateral walls by the upper and lower alveolus covered by gingival mucosa, and the floor which is chiefly formed by the mylohyoid muscle. The vestibule is a cleft lined by the buccal mucosa laterally, superiorly and inferiorly by reflections of the buccal mucosa onto the mandible and maxilla, respectively, referred to as the upper and lower gingivobuccal sulci (GBS), the gingival mucosa medially [Figure 1], the lips anteriorly and leads to the retromolar trigone posteriorly.

The retromolar trigone (RMT) is a mucosal fold extending behind the mandibular last molar along the ascending ramus of the mandible upto the maxillary last molar on either side [Figure 2]. It is triangular in shape with base behind the mandibular last molar and apex at the maxillary tuberosity.[2] Beneath the mucosal fold lies the pteryomandibular raphe that attaches superiorly to the pterygoid hamulus and inferiorly to the posterior end of the mylohyoid line. On CT images the RMT is seen in two or three consecutive axial sections, the upper limit behind the maxillary last molar and the lower limit behind the mandibular last molar. The RMT can be seen in its entirety in the oblique plane that can be reformatted with MDCT [Figure 2A].

Lateral to the buccal mucosa is the buccomassteric region or buccal space which though not a part of the oral cavity needs mention. Squamous cancers arising from the buccal mucosa often spread to this region and beyond into the masticator space upstaging disease. The buccomasseteric region is bounded by the buccinator medially and the zygomaticus major laterally while the masseter is located posteriorly [Figure 3]. It consists of the buccal fat, angular branch of the facial artery, facial vein, buccal artery, nerves (not identified on imaging), the terminal part of the parotid duct and the facial node. Superiorly this space leads to the masticator space with often incomplete fascial boundaries between.

The oral tongue located in the central part of the oral cavity is composed of numerous muscles wrapped in mucous membrane. It is formed by the anterior two-thirds of the tongue upto the circumvallate papillae while the posterior one-third of the tongue, also called base tongue is a part of the oropharynx. The midline lingual septum divides the tongue into equal halves, consisting of the intrinsic and extrinsic muscles.

The four intrinsic muscles which form the bulk of the tongue are superior and inferior longitudinal, transverse and vertical. These interdigitate with each other in the upper portion of the tongue. They are difficult to appreciate on CT, but are well seen on MR imaging[3] [Figure 4]. The
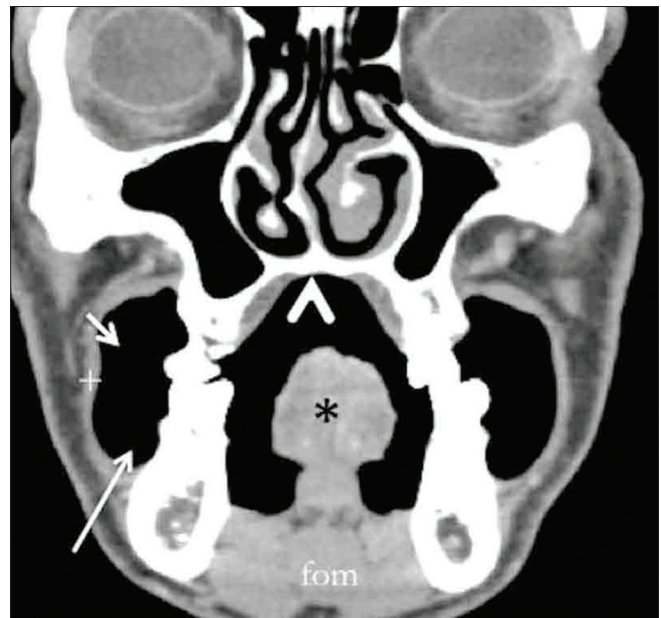

Figure 1: Coronal MDCT reformation with puffed cheek technique showing oral cavity proper with tongue (asterisk), vestibule (short arrow), lower gingivobuccal sulcus (long arrow), hard palate(^) and buccal mucosa closely apposed to buccinator (+)
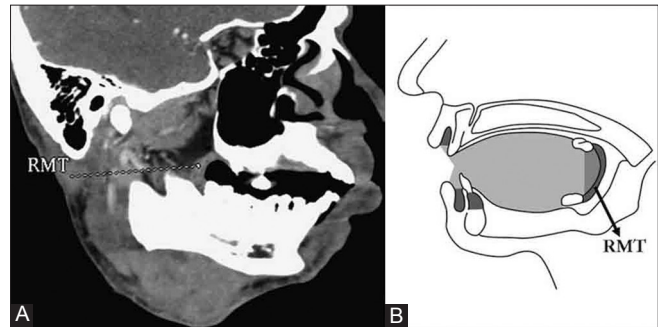

Figure 2 (A, B): (A) Oblique reformation on a 16 slice MDCT scanner depicting the anatomy of retromolar trigone. (B) Line diagram showing the same
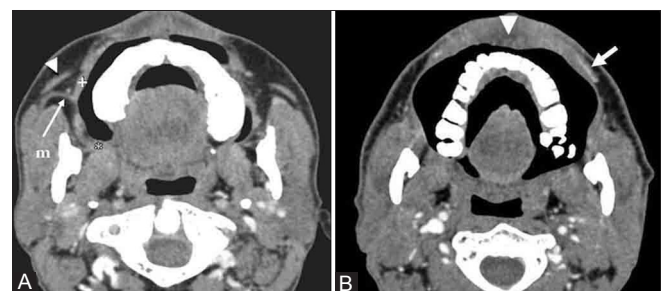

Figure 3 (A, B): Illustrates (A) Buccomasseteric region bounded by zygomaticus major (arrowhead), masseter(m), buccinator (+) inserting into pterygomandibular raphe (*) and terminal parotid duct(arrow). (B) Shows orbicularis oris (arrowhead) and levator anguli oris (arrow)

four extrinsic muscles of the tongue are genioglossus, hyoglossus, styloglossus and palatoglossus, best seen on T2W MR images. They provide attachment of the tongue to hyoid bone, mandible and styloid process. The largest

is the fan-shaped genioglossus that originates from the superior genial tubercle, located on the inner aspect of midline mandible and fans out superiorly to interdigitate with the intrinsic muscles. Inferiorly it attaches to the body of hyoid bone. It is well seen on sagittal, coronal and axial MR images [Figures 4 and 5]. The hyoglossus are thin flat quadrilateral muscles that course lateral to the genioglossus from the greater cornua of the hyoid bone to the sides of the tongue. The hyoglossus is best appreciated on axial and coronal MR imaging [Figures 6A and B]. The palatoglossus muscle covered by the mucosa forms the anterior tonsillar pillar. It arises from the oral surface of the soft palate and passes anterior to tonsil and downward to blend with the hyoglossus and may not always be appreciated on imaging[3] [Figure 7A]. The styloglossus arises from the styloid process and stylomandibular ligament, passes forwards and interdigitates with the hyoglossus [Figure 7B].

The floor of the mouth (FOM) is formed primarily by the mylohyoid which is a U-shaped sling extending from one mylohyoid ridge on the inner aspect of the mandible to the other ridge. Anteroposteriorly it extends from the symphysis menti to the last molar tooth. It inserts both into the midline fibrous raphe and the hyoid bone and is best seen on coronal planes on both CT and MR imaging [Figure 8]. The submandibular gland is located inferior to the mylohyoid [Figure 7A]. The deep lobe of the submandibular gland wraps around the posterior free border of mylohyoid to lie on the superior surface of the mylohyoid. However, surgically the FOM is the space between the mucous membrane of the FOM and the mylohyoid.[3]

Two other muscles, geniohyoid and anterior bellies of digastric support the FOM. The paired geniohyoid arising from the inferior genial tubercles run above the mylohyoid in a paramedian position to insert into the hyoid.[3] They are seen best in the sagittal plane on MR images as darkly hypointense structures on T2W images [Figures 8 and 9A]. The anterior bellies of digastric are seen on the inferior surface of the mylohyoid, best seen on the coronal plane [Figure 8].

The sublingual space (SLS) is seen superomedial to the mylohyoid and lateral to the genioglossus [Figures 6A and 9B].[3] It is a fat-filled space and contains the sublingual gland, deep part of submandibular gland, Wharton's duct, lingual neurovascular bundle [Figure 10A] and the anterior fibers of hyoglossus. On CT it appears as a low density plane [Figure 10B] while on MRI it is seen as a hyperintense area [Figure 9B].
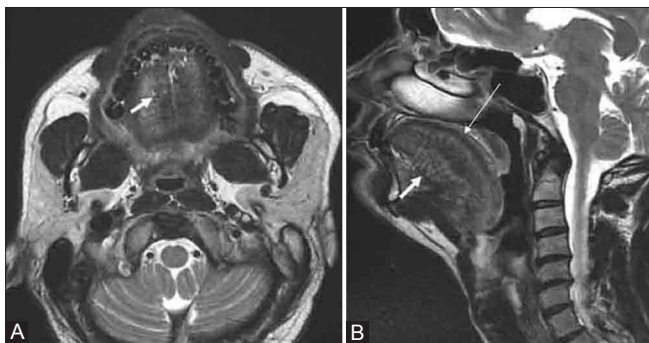

Figure 4 (A, B): (A) Axial T2 W MRI shows intrinsic muscles (arrow) at the level of dorsum tongue. (B) Sagittal T2W MRI showing the fan-shaped genioglossus(short thick arrow) and the longitudinal intrinsic muscle (long thin arrow)
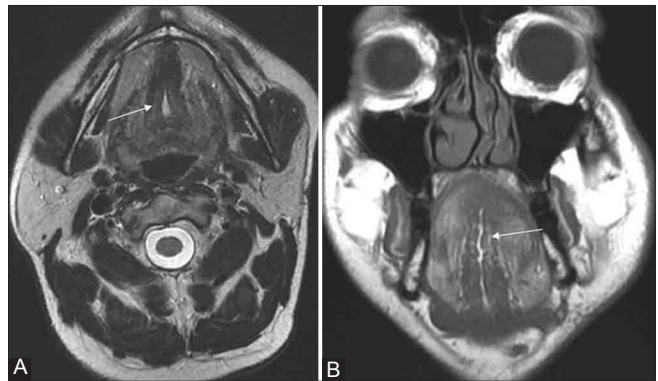

Figure 5 (A, B): (A) Axial T2W MRI showing the paired genioglossus (arrow) on either side of midline at the level of mandibular alveolus. (B) Coronal T1W MRI showing genioglossus (arrow)
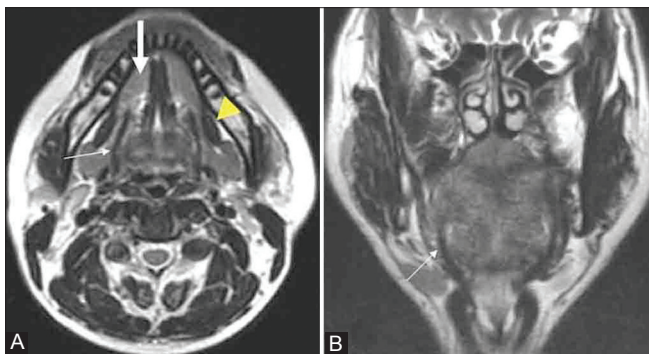

Figure 6 (A, B): (A) Axial T2W MRI showing hyoglossus (thin arrow), mylohoid (arrowhead), the hyperintense sublingual space (thick arrow) and (B) Coronal T2W MRI showing hyoglossus (thin arrow)
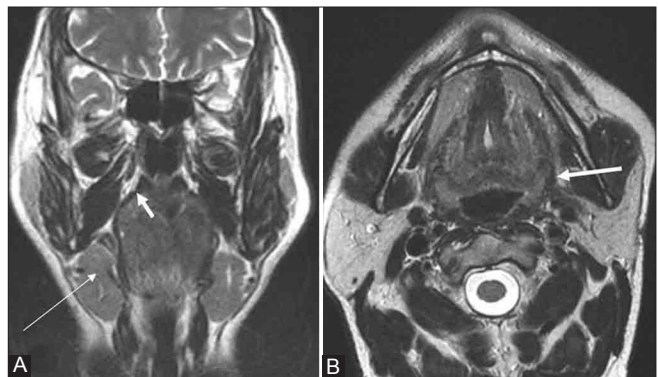

Figure 7 (A, B): (A) Coronal T2W MR image showing palatoglossus (thick arrow), submandibular gland (long arrow) and (B) Axial T2W MR image showing the styloglossus (thick arrow)
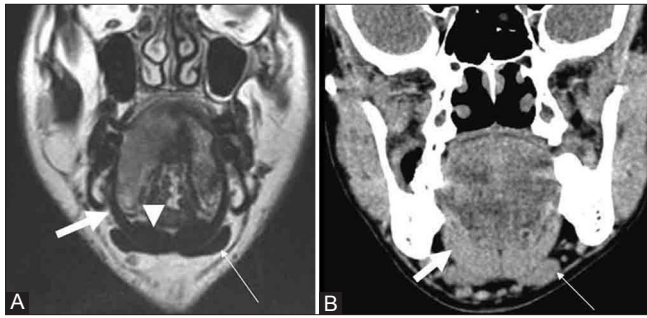
Figure 8 (A, B): (A) Coronal T2W MRI and (B) Coronal CT reformat show U-shaped sling of the mylohyoid (thick arrows). Thin arrows point to the anterior belly of digastric. Arrowhead in A points to geniohyoid. All three comprise radiological floor of mouth
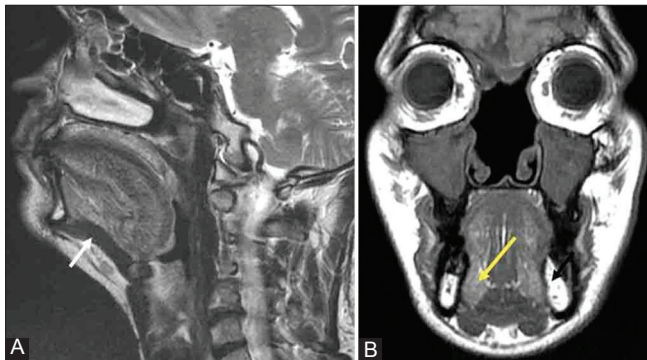

Figure 9 (A, B): (A) Sagittal T2W MR image showing darkly hypointense geniohyoid (arrow) from genial tubercle to hyoid. (B) Coronal T1W MRI showing the fat-filled sublingual space (arrow)
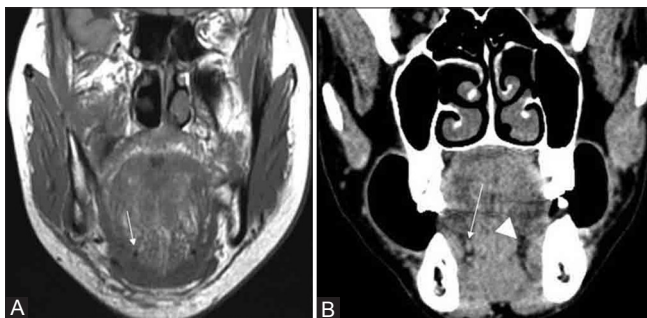

Figure 10 (A, B): (A) Coronal T1W MR image showing lingual artery in sublingual space (arrow). (B) Postcontrast coronal CT reformation showing fat-filled sublingual space on the left (arrowhead) with lingual artery visible on the right (thin arrow)

Management of Oral Cancers

Oral cavity comprises of several subsites, which are the lips, buccal mucosa, upper alveolus with gingiva, lower alveolus with gingiva, RMT, oral tongue (anterior two-thirds), FOM and hard palate. Management of oral cavity SCC depends on the stage of disease.[4,5] Stage I and II cancers (T1-T2, N0) are treated with single modality therapy, surgery or radiotherapy (RT) for the primary, the former being favored. Management of the neck is discussed in the section on neck node metastases. Locally advanced

cancers (Stage III and IV) are treated with combination of surgery, radiotherapy and chemotherapy for both primary and the neck.

The 7th edition of AJCC (2010) staging for oral SCC[5] is provided in Table 1. The radiologist should be familiar with T4a (moderately advanced) and T4b (very advanced) subcategories of T4 and provide information indicating T stage and N stage of disease to the clinician. In addition few other specific issues need mention at various subsites that will be dealt in the respective sections.

Gingivobuccal and RMT SCC

Gingivobuccal SCC include those arising from the buccal mucosa, the gingival mucosa covering the upper and lower alveolus and from the gingivobuccal sulci (together called the gingivobuccal complex). SCC of the lower gingivobucccal complex are the most common oral cancers in the Indian subcontinent due to tobacco chewing and have been described as the " Indian oral cancer".[6]

Important issues in gingivobuccal and RMT SCC that have an impact on management and prognosis are soft tissue spread, bone erosion and nodal involvement.[7,8] At our institute very early SCC which are seen as superficial ulcers on the buccal mucosa are not imaged for the primary, but are referred for ultrasound evaluation of the neck for nodal status. An ulcerous lesion on the gingival mucosa, however, requires cross-sectional imaging to rule out bone erosion.

All other SCC require more detailed evaluation by imaging. CT and MRI perform comparably for assessment of soft tissue extent,[9-11] but CT is preferred for evaluating bone erosion.[12,13] Although several reports have evaluated PETCT in the initial staging of oral cavity SCC, the diagnostic yield of PETCT did not score over anatomical imaging for either the evaluation of the primary or occult nodal metastasis[14,15] and we do not use it in the initial evaluation of oral SCC. However, the NCCN guidelines suggest a level 2A evidence for use of PETCT in stage III- IV disease that could alter management by demonstrating distant metastases.[5]

Contrast-enhanced multidetector computed tomography (MDCT) combines the advantages of speed of scanning and the ability to use the "puffed cheek" technique for imaging gingivobuccal and RMT cancers [Figures 1 and 11]. A 16-slice MDCT scanner provides adequate thin slices for isotropic coronal, sagittal and oblique reformations. Bone and soft tissue algorithms are obtained. Puffed cheek technique requires the patient to blow uniformly through pursed lips while breathing normally.[16] The technique can be improved further by pushing the tongue away from the hard palate.[17]

Table 1: AJCC 7th edition 2010 (TNM classification)

Tumor

  TX- Primary tumor cannot be assessed

  T0- No e/o primary tumor

  Tis- Carcinoma *in situ*

  T1-2 cm or less

  T2 - >2 cm but ≤4 cm

  T3 - >4 cm

  T4a (Oral cavity)-Moderately advanced local disease-Invades through cortical bone, into deep (extrinsic) muscles of tongue, maxillary sinus, or skin of face

  T4b-Very advanced local disease--Involves masticator space, pterygoid plates, or skull base or encases internal carotid artery

Node

  NX-Cannot be assessed

  N0-No regional lymph nodes metastasis

  N1-Single ipsilateral lymph node, <3cm in greatest dimension

  N2

    N2a-Single ipsilateral lymph node, 3-6 cm in greatest dimension

    N2b-Multiple ipsilateral lymph nodes, ≤6cm in greatest dimension

    N2c-Bilateral or contralateral lymph nodes, ≤6cm in greatest dimension

  N3-Lymph node(s) >6 cm in greatest dimension
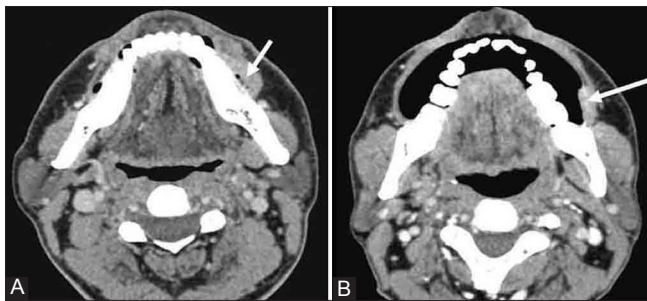
Metastasis

  M0-none

  M1-yes

Figure 11 (A, B): (A) Axial CECT showing the Puffed Cheek technique in (B) that separates the buccal and gingival surfaces with air depicting that epicenter of lesion (arrows) is in the buccal mucosa .The lesion does not abut mandible as appears in A

Figure 12 (A, B): CT shows (A) Squamous cancer in the upper GBS eroding floor of left maxillary sinus(arrow) and laterally invading skin (*). (B) Advanced buccal SCC with lateral spread to skin and orocutaneous fistulation(arrow). Posteriorly adherent to masseter (m)

Soft tissue extension

Gingivobuccal SCC can spread laterally into the overlying buccal and subcutaneous fat upto the skin, superiorly into the maxillary sinus [Figure 12], medially erode the mandible and extend across into the lingual musculature all of which are defined as Stage T4a.[5] They can extend anteriorly into the lips and occasionally spread perineurally through the mental foramen. Postero-superior spread into the masticator space is classified as T4b.[5]

Involvement of the skin is a clinical finding documented by induration and peau d'orange appearance requiring appropriate reconstruction following resection. This could appear as stranding of the subcutaneous fat on CT and needs mention. However, Spector, *et al*. noted in a small series that linear reticulations seen on CT in the dermis and subcutaneous fat adjacent to the tumor were more
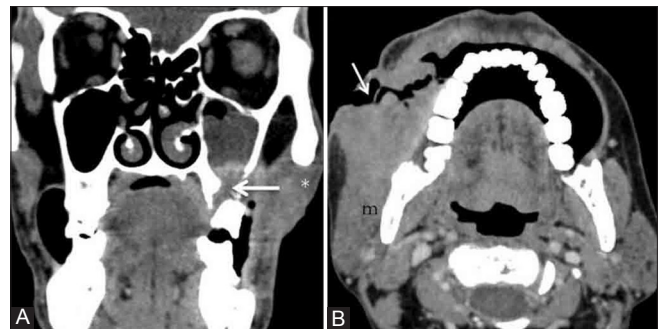
often due to peritumoral inflammation rather than tumor invasion.[18]

Postero-superior spread: Although the AJCC 6th edition called masticator space involvement (T4b) unresectable, the 7th edition reclassifies this as very advanced disease. This is because some cases with masticator space involvement may be amenable to resection, while involvement of the skull base and internal carotid artery is definitely unresectable. A recent report compared the outcomes of resection of advanced buccal SCC that had spread to the masticator space. The mandibular notch between the coronoid and conyloid process was used as a line of demarcation and disease classified as supra-notch and infranotch.[19] A subset of T4b with infranotch disease were found to have a more favorable prognosis (local control of 74%) than those with

supranotch disease (local control of 42.9%). The distance between the skull base and mandibular notch is 2 cm while the distance between skull base and lower limit of pterygoid plates is 3 cm.[19] Hence the upper part of the pterygoid plates are a supranotch structure while their lower limits are in the infranotch compartment. While seeking information regarding posterior spread, some clinicians are more familiar with the term infratemporal fossa (ITF). The *masticator space* (MS) well known to the radiologist refers to the compartment formed by splitting
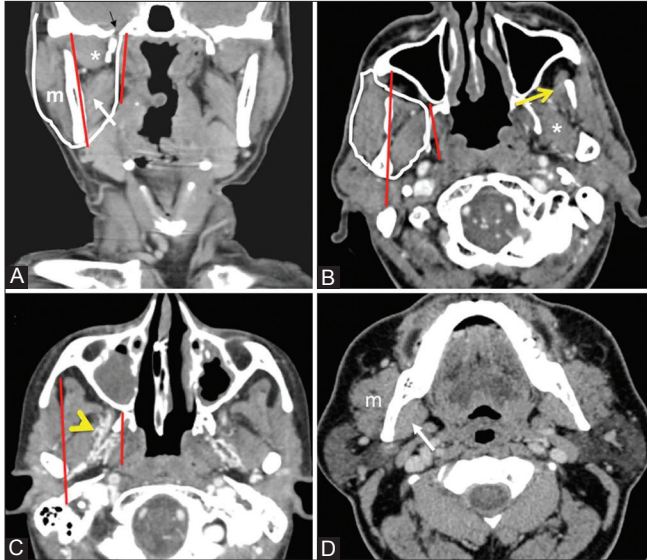
of the layers of the investing layer of cervical fascia at the lower border of the mandible. It contains the ramus and posterior body of mandible, masseter, temporalis, medial and lateral pterygoid muscles and the mandibular division of trigeminal nerve, which continues as the inferior alveolar nerve (within the mandible).[3]Although MS and ITF are often used synonymously in the current lexicon for reasons described below, some mention is needed of the subtle difference. The *ITF* [Figure 13 A-C] is a non fascial lined space bounded anteriorly by the posterior surface of the maxilla, posteriorly by the mastoid temporal bone, superiorly by inferior surface of greater wing of sphenoid and squamous temporal bone, laterally by the inner surface of vertical ramus of mandible, and medially from anterior to posterior by the sphenoid pterygoid process, pterygomaxillary fissure and lateral wall of nasopharynx.[20,21] Inferiorly the anatomical fossa has no floor and ends at the level of angle of mandible.[20] The major contents of the ITF are pterygoid muscles, internal maxillary artery, pterygoid venous plexus [Figure 13C], and mandibular division of trigeminal nerve. The masseter is not a content of the ITF. The ITF thus combines the medial part of the masticator space, part of the parapharyneal space and the retroantral buccal space. The inferior and superior boundaries of both spaces are at the same levels with the foramen ovale seen in the roof [Figure 13A].

Irrespective of the terminology used, in oral cavity SCC it is important to precisely convey the craniocaudal extent of disease spread. Spread of disease into the upper part of the space closer to skull base (high ITF or high masticator space or supranotch disease) constitutes a section of T4b SCC with unfavorable surgical outcomes and surgical morbidity

Figure 13 (A-D): ITF and MS. White outlines in A & B define MS. The red lines in A, B & C enclose ITF. B & C show supranotch ITF. D. shows low masticator space (infra-notch level). Note lateral pterygoid (*), medial ptergoid (white arrow), masseter (m), foramen ovale (black arrow), temporalis (yellow arrow), and pterygoid venous plexus (arrowhead in C) in the parapharyngeal part of ITF

Figure 14 (A, B): (A) Coronal CT reformat showing squamous carcinoma with high masticator space invasion (*), (+) shows normal opposite lateral pterygoid. (B) Bone window. Arrows in A and B show widened foramen ovale with enhancement in A (perineural spread)

[Figure 14]. The normal high space is easily identified on axial imaging as containing the lateral pterygoid muscle and the upper two-thirds of pterygoid plates [Figure 13B] while the low masticator space contains medial pterygoid and masseter muscles [Figure 13D]. Disease involving low masticator space/low ITF or infranotch compartment comprises a subset of T4b SCC with favorable surgical outcomes and most clinicians prefer to operate this group [Figure 15A and B].

Perineural spread through the foramen ovale may occur and causes foraminal widening on CT [Figure 14]. Perineural spread is, however, best imaged on MRI and may be seen as excessive enhancement within foraminae or loss of normal fat density.[22] RMT SCC can spread to several sites, both circumferentially and superiorly as illustrated in Figures 16 and 17.
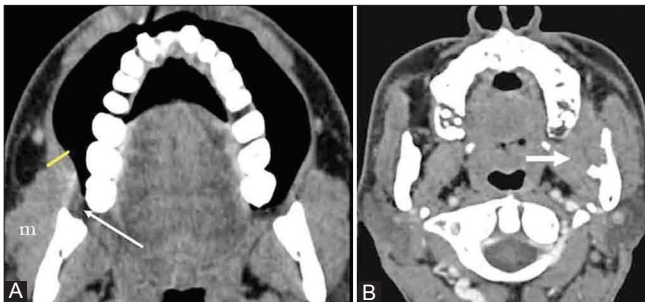

Figure 15 (A, B): Showing two buccal cancers in low masticator space. (A) shows squamous carcinoma in posterior right buccal mucosa (yellow line) reaching RMT (arrow), invading masseter(m). (B) Arrow shows left medial pterygoid invasion and erosion of vertical mandibular ramus
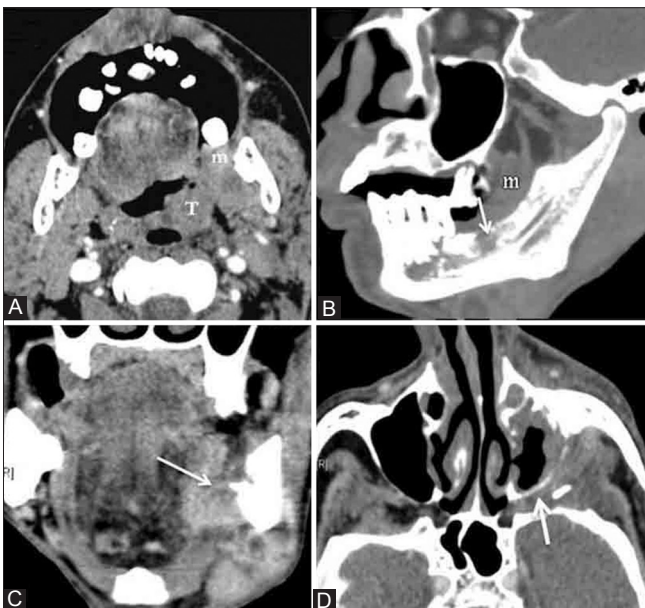

Figure 17 (A-D): RMT cancers (m) (A) showing extension along pterygomandibular raphe to tonsil (T) (B) Oblique reformat showing mandibular invasion (arrow) (C) Mandibular erosion and tongue invasion (arrow) (D) Superior spread to pterygopalatine fossa (arrow) seen as loss of normal fat density

Bone erosion and role of various imaging modalities

Bone erosion by SCC is an adverse prognostic criterion and requires some form of mandibular resection, either marginal or segmental mandibulectomy [Figures 18A, B]. Marginal mandibulectomy involves resection of a part of the superior rim of the mandible. It requires preservation of an at least 1 cm vertical height of the body of the mandible for strength. It ensures that mandibular continuity is maintained and a much better cosmetic and functional end result is achieved. It is offered when subtle erosion is present or when a small soft tissue component abuts the mandible without causing erosion.[6,23,24] Segmental mandibulectomy is performed when there is gross erosion and invasion of the inferior
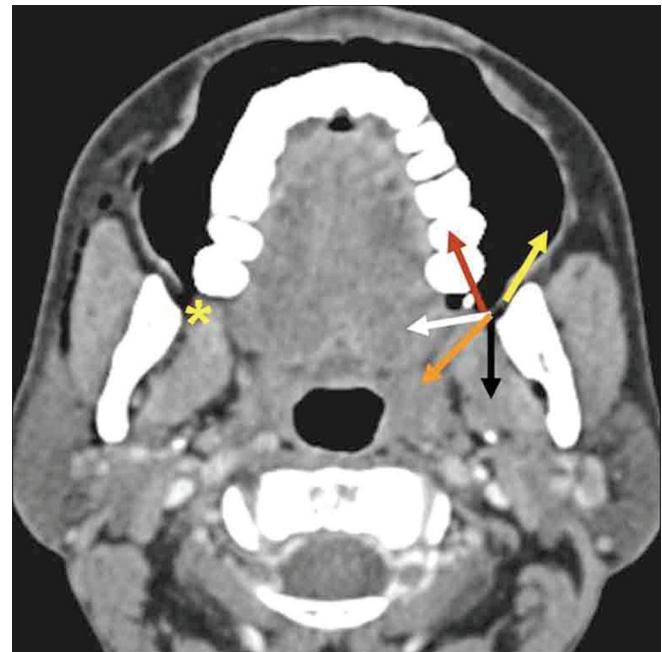

Figure 16: Shows possible pathways of spread of RMT cancers, Buccal mucosa (yellow arrow), maxillary and mandibular alveolus (red arrow), Base tongue/FOM (white arrow), tonsil (orange arrow), masticator space (black arrow), and through pterygomandibular raphe (*) superiorly to pterygopalatine fossa
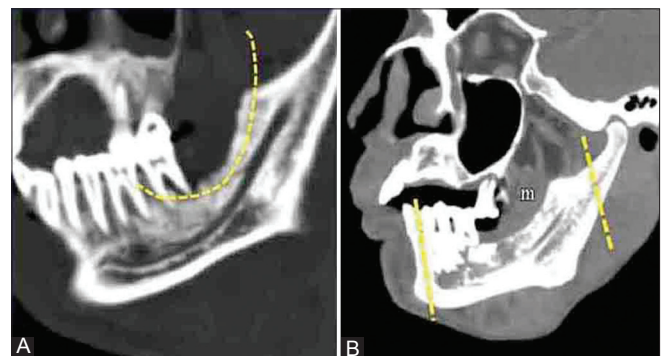

Figure 18 (A, B): Oblique reformations on 16 slice MDCT scanner, bone windows (A) shows incision line of marginal mandibulectomy (rim resection above inferior alveolar canal) and (B) Incision lines for segmental mandibulectomy (which includes mental foramen and spares conyloid process)

alveolar canal [Figure 19A], extensive paramandibular soft tissue spread [Figure 19B], in edentulous mandibles (where the height is inadequate) and in irradiated mandibles.[6]

Preoperative imaging needs to comment on absence or presence of mandibular erosion, whether erosion is subtle or gross (buccal, occlusal, and/or lingual cortices and if the marrow and inferior alveolar canal are invaded). The anteroposterior extent of erosion (on axial images) and the height of the uninvolved segment of mandible from the inferior border (on coronal imaging) need to be recorded to plan marginal mandibulectomy [Figure 20]. The oblique reformation best depicts the inferior alveolar canal in the lateral segment of the curved mandible [Figures 18 and 19A]. Reformations done ad hoc on workstations or on the PACS with spatial cursor localization facilitate confident assessment. Imaging should record sparing of the condyloid process and posterior segment of the mandible which helps plan reconstruction, necessary after segmental mandibular resection.

Numerous prospective and retrospective studies have investigated various imaging methods such as orthopantomogram (OPG), CT scan, Denta scan, MRI, Bone scan and SPECT for assessing mandibular invasion in oral squamous cancers. Comparison has also been made with clinical examination and periosteal stripping. Although initially imaging was pronounced inaccurate as compared to clinical examination, subsequent studies conclusively proved the role of imaging in assessing mandibular invasion. CT was found to have the highest specificity (87%) while SPECT and MRI had the highest sensitivity (96-97%).[9,25-33] Two studies have also evaluated MDCT and found a sensitivity of 82.6 % and specificity of 86.9% for mandibular invasion.[34,35] Vidiri, *et al*. found no statistically significant difference in accuracy between MRI and MDCT,[34] while another study by Imaizumi, *et al*. showed that MRI overestimated mandibular cortical erosion and inferior alveolar nerve involvement[13] [Figure 21]. Disadvantages with OPG include inability to image soft tissue, false positives due to periodontitis, inability to assess the symphysis menti region and visibility of erosion only after 30-75% mineral loss.[25] Table 2 provides a checklist for reporting in gingivobuccal and RMT SCC.

Tongue and Floor of Mouth SCC

There is a rising incidence of oral tongue SCC both in India and in the West. This is associated mainly with tobacco and alcohol use, but a small proportion have been associated with HPV infections.[36] Squamous cancers of the oral tongue behave differently from those of the base tongue which are similar to oropharyngeal cancers. This review focuses on oral tongue SCC, the majority of which arise from the lateral border with few from the ventral surface. Imaging for tongue SCC requires a modality with superior
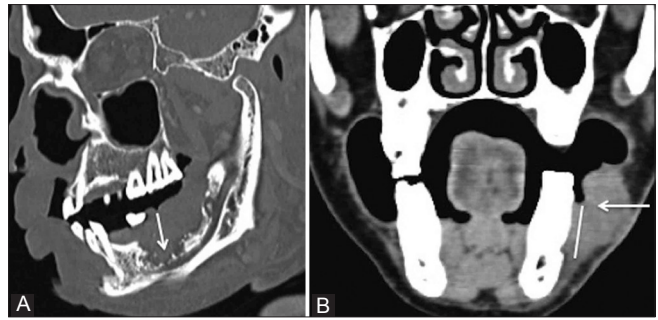

Figure 19 (A, B): Indications for segmental mandibulectomy. (A) Oblique MDCT reformation showing extensive mandibular erosion reaching inferior alveolar canal (arrow) (B) Large paramandibular soft tissue mass (arrow) seen on coronal reformat CECT abutting a large surface of mandible (vertical line) without eroding
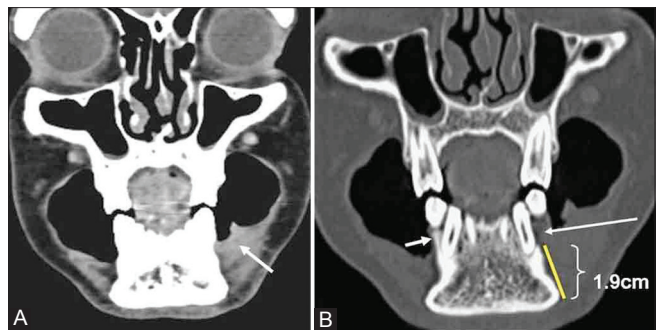

Figure 20 (A, B): (A) Lower GBS mass abutting mandible (arrow) (B) Coronal reformat (bone algortithm) shows subtle erosion of buccal cortex (long arrow). Short arrow shows opposite intact cortex. Yellow line shows adequate height of uninvolved mandible (at least 1cm to prevent fracture)
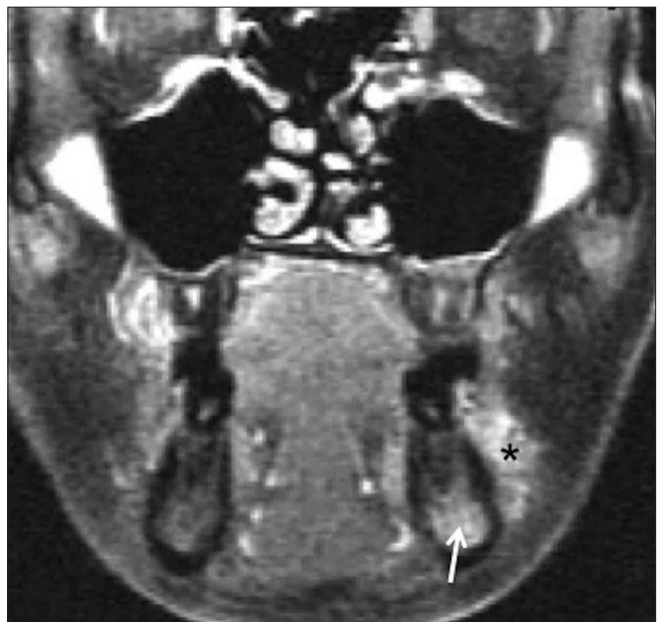

Figure 21: Overestimation by MRI. Coronal contrast enhanced MRI shows an enhancing lower gingivobuccal SCC (*) and suspected perineural spread along inferior alveolar nerve (arrow shows enhancement). Postsegmental mandibulectomy histopathology revealed nerve to be free of disease

Table 2: Gingivobuccal and RMT cancers

Imaging Modality—Contrast-enhanced MDCT with puffed cheek technique (one-stop shop for soft tissue, bone and nodes)

Checklist

Epicenter and dimensions

Soft tissue extent (lateral, superior and medial)—overlying skin, maxillary sinus, paramandibular extent, lingual muscles, BOT and FOM (T4a)

Soft tissue extent—posteriorly to RMT, pterygomaxillary fissure, pterygopalatine fossa, pterygoid plates and masticator space/ITF (T4b) with supra or infra mandibular notch extent.

Bone erosion and extent—mandible(height and AP extent) and maxilla.

Nodal status—number & size of abnormal nodes, level, presence of necrosis/extracapsular spread, invasion of adjacent structures and vessels.

soft tissue characterization and hence MRI is the optimal modality, displaying exquisite anatomical detail including intrinsic and extrinsic muscles, the floor of mouth (FOM) and the lingual vascular bundle.[37-39] CT has insufficient soft tissue characterization and is frequently hampered by dental artefacts.

An optimal MR imaging protocol is incomplete without postgadolinium T1W sequences as the tumor frequently shows intense enhancement and is best depicted on this sequence[40] [Figure 22]. Our protocol on a 1.5 T magnet using a head and neck phased array coil is acquired with axial and coronal spin-echo T1-weighted (TR, 500-600 ms; TE, 7-10 ms); axial and sagittal fast spin-echo T2-weighted (TR, 3000-4000 ms; TE, 90-100ms); coronal short tau inversion recovery (STIR) (inversion time, 150 ms); and postcontrast axial, coronal, and sagittal T1-weighted sequences. The sequences are acquired at 4-mm thickness with 1-mm intersection gap. The matrix used is 256×256, NEX 2 and FOV 240 mm. Echoplanar diffusion weighted imaging is performed with b values of 0 and 1000 sec/mm^2.

Noncontrast T1W sequences demonstrate cortical erosion and marrow invasion. Contrast-enhanced T1W images help assess marrow invasion,[13] perineural spread, soft tissue extent, tumor thickness and best demonstrate necrosis in nodes. T2W sequences depict extrinsic muscle and FOM involvement as well as nodes.[40] STIR images have high sensitivity for visualizing nodes but with reduced specificity. DW images are of added value, particularly in subcentimeter metastatic nodes.

In oral tongue SCC seen as very shallow ulcers, imaging may not be required for the primary, but due to a high incidence of occult cervical lymph node metastasis[5,41] the neck needs investigation with ultrasonography. In early tumors, the important issue is tumor thickness which has prognostic relevance. A tumor thickness of >4 mm on histopathology (HP) has been associated with increased incidence of cervical nodal metastases.[42]
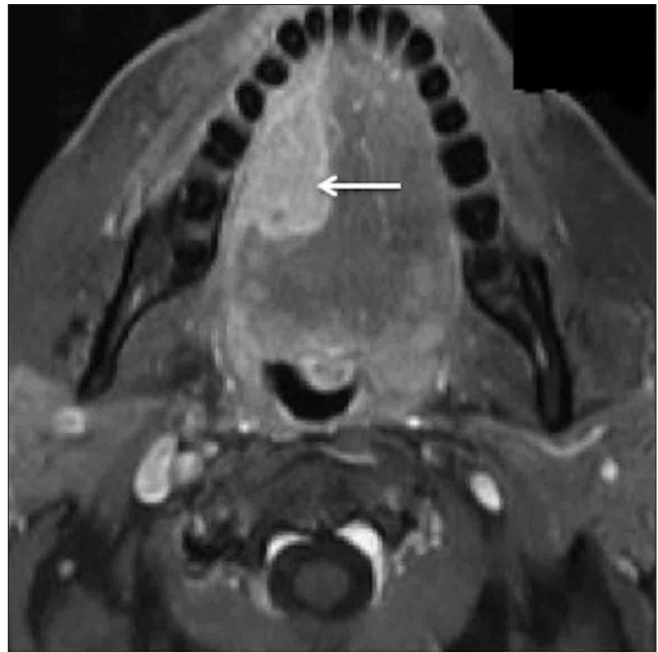
The value of MRI in staging and measuring the tumor

Figure 22: Axial contrast-enhanced T1W MRI best depicts a SCC arising from right lateral border of oral tongue that shows intense enhancement (arrow)
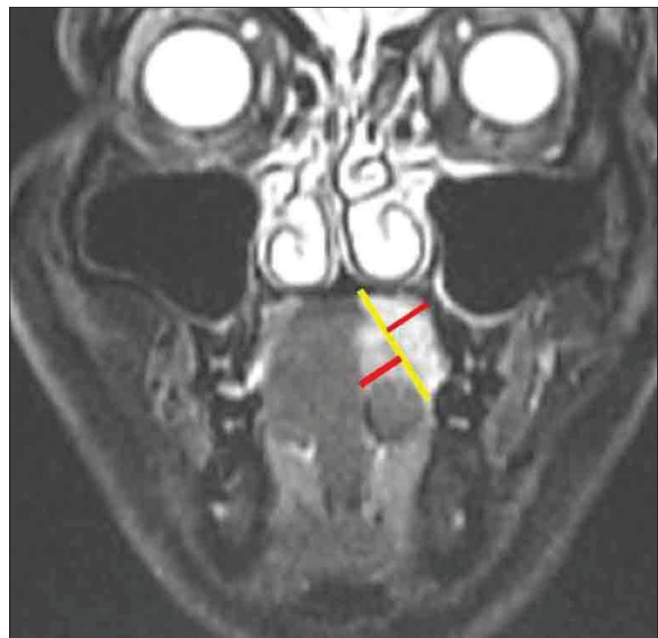

Figure 23: Coronal STIR image showing left tongue carcinoma. Yellow line represents reference line drawn between the two tumor mucosa junctions. Perpendicular measurements (red lines) on either side to the point of maximal tumor projection are added to get tumor thickness

thickness has been established.[43-46] Figure 23 depicts measurement of tumor thickness[45] which is a latero-medial and not a craniocaudal dimension for the vast majority of tumors that arise from the lateral border. Lam, *et al.* found a higher concordance rate for tumor thickness using contrast-enhanced T1W images (83%) than with T2W images (56%) due to peritumoral inflammation seen

as hyperintensity with the latter.[45] Okura, *et al.* evaluated the features of primary tongue SCC on MR imaging to predict cervical nodal metastases and found that a tumor thickness of >9.7 mm was a significant predictor for nodal metastases and proposed that elective neck dissection could be performed in such cases.[47] Intra-oral ultraonography has also been used successfully for measuring tumor thickness.[48,49]

MRI can also accurately depict the T stage, another factor with bearing on prognosis and treatment. Extension to the extrinsic muscles (upstaging disease to T4a), encasement of neurovascular bundle, invasion of the FOM and base tongue are well seen [Figures 24 and 25]. These features influence the choice of therapy (single or multiple modality) and the extent of surgical resection that can vary from wide excision to partial glossectomy to total glossectomy (for tumors involving bilateral neurovascular bundles). The latter procedure can be morbid with poor outcome and often such patients are offered organ preservation therapy (chemotherapy followed by concurrent chemoradiation). Extension of primary tumor upto or across the midline may require bilateral neck dissection or irradiation to address ipsilateral and contralateral neck node metastases [Figure 24B]. Extension to valleculae, pre-epiglottic space and hyoid bone [Figure 25] need to be documented as they are relative contraindications to surgical treatment. This is because removal of hyoid would require at least a supraglottic laryngectomy that necessitates more extensive reconstruction increasing morbidity. Extension to tonsil and lateral pharyngeal wall are also relative contraindications. Therefore precise soft tissue extent depicted by imaging has a significant impact on management. Bone erosion can occur in tongue SCC extending to FOM or primary FOM cancers although seen less frequently than in buccal cancers [Figure 26]. Involvement of the segment of the involved mandible (midline or lateral) needs to be recorded with detailed information as described earlier. Midline invasion of the genial tubercles leading to mid-third mandibulectomy can result in loss of tongue and laryngeal muscle attachments, requiring appropriate reconstruction. Imaging can also assist plan adequate reconstruction after resection. When the tumor involves geniohyoid and mylohyoid, the entire thickness of the FOM needs extensive reconstruction with an anterolateral thigh flap or pectoralis major myocutaneous flap. Involvement of parts of genioglossus and hyoglossus alone can be reconstructed with free radial artery forearm flap [Figure 27]. Table 3 provides a checklist for reporting in oral tongue and FOM cancers.

Neck node metastases

Involvement of a single node reduces survival by half.[50] Gingivobuccal and tongue SCC initially spread to level I and II nodes respectively. Skip metastases with tongue cancers to level III and IV and to contralateral I and II levels
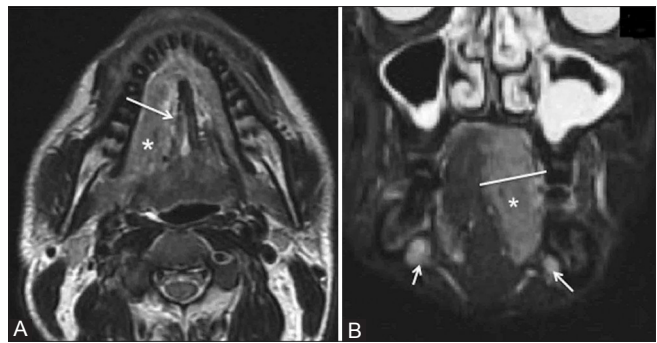

Figure 24 (A, B): (A) Axial T2W MRI (B) Coronal STIR MRI show hyperintense tongue SCC (*) in two different patients invading genioglossus (arrow in A) B. Lesion crosses midline (white line) and bilateral metastatic IB nodes seen (short arrows)

Figure 25: Sagittal contrast-enhanced MRI shows an enhancing tongue SCC (*) reaching FOM (arrowhead), base tongue and valleculae (long arrow) and invading the mandible (short arrow)

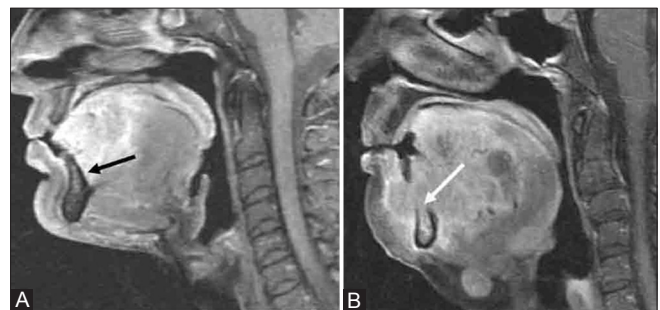

Figure 26 (A, B): (A) Bulky enhancing tumor in anterior tongue abutting lingual cortex of mandible which is intact (arrow) (B) Bulky tumor in another patient with erosion of occlusal cortices of mandible and enhancement in the marrow (arrow)
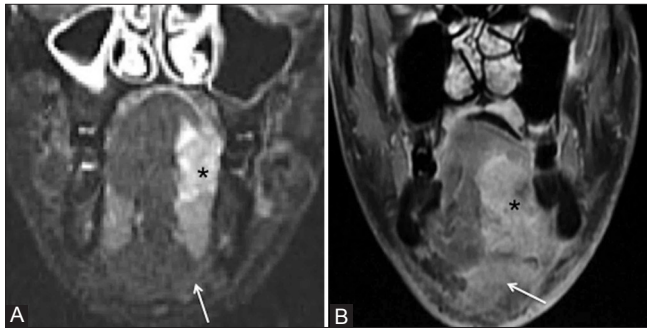
Figure 27 (A, B): (A) Coronal STIR MRI shows tongue SCC (*) reaching upto sublingual space sparing mylohyoid (arrow) (B) Coronal contrast-enhanced fat-suppressed T1W MRI shows enhancing tongue SCC (*) invading mylohyoid (arrow)

are also known. When the neck is negative for nodes on clinical examination, it is referred to as the cN0 (clinically negative) neck while the cN+ (clinically positive) neck refers to palpable neck nodes. However clinical examination is unreliable for detection of nodes and the incidence of occult neck nodal metastases even in early oral cancers varies from 16% to 40% in tongue cancers.[41,42]

The cN+ neck is addressed with modified radical neck dissection. In the cN0 neck, elective neck dissection was proposed when the incidence of nodal metastases was greater than 15-20%.[42] A recent meta-analysis proposed it for all cN0 necks in oral cancers,[51] but the meta-analysis was criticized.[52,53] A meta-analysis has analyzed numerous
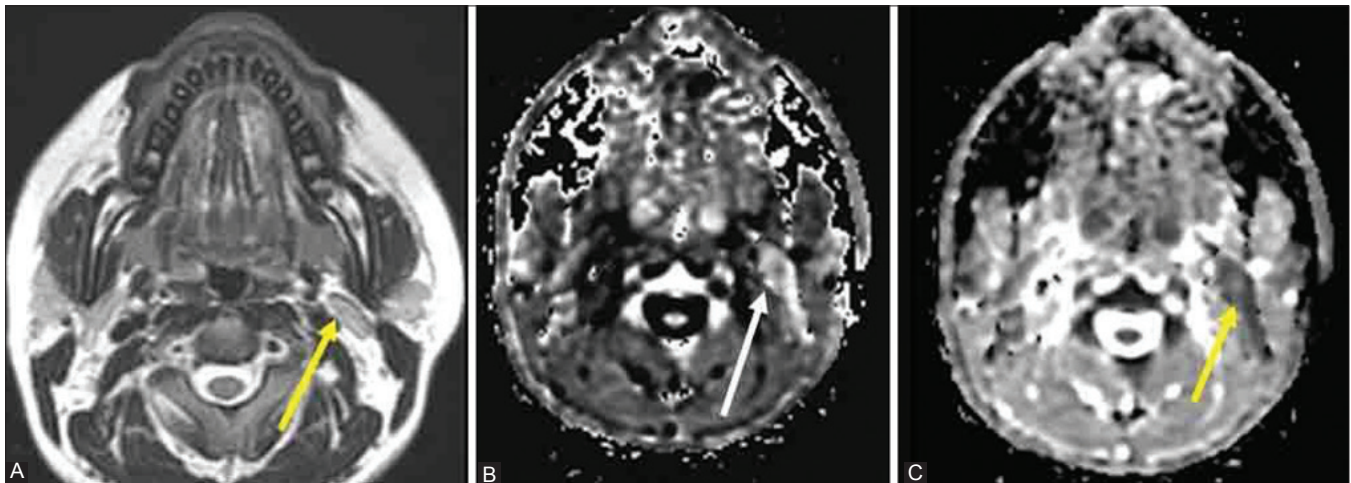

Figure 28 (A, B): Metastatic left level II node. Arrows show (A) Node on Axial T2W MRI with no abnormal features (B) Hyperintense lymph node on b =1000 sec/mm^2 (C) The transverse ADC map with hypointensity in same node (ADC of 0.84 x 10-3 mm^2/sec)
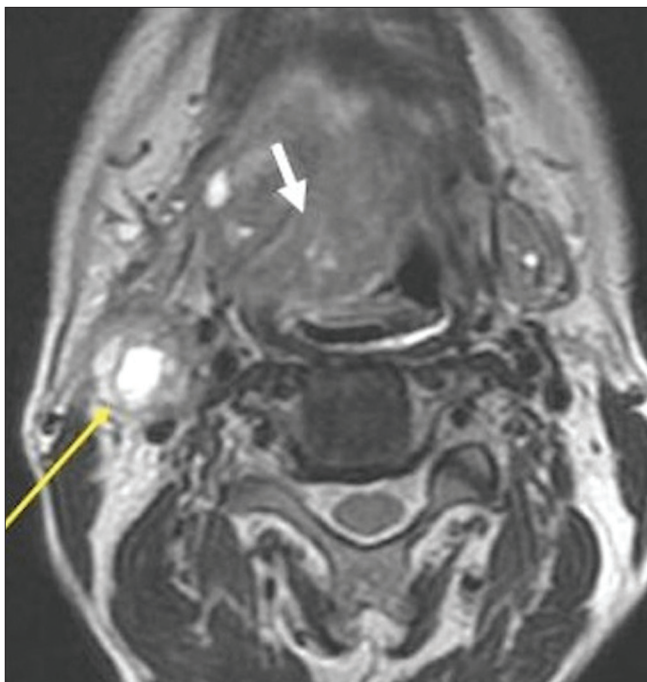
Figure 29: Axial T2W MRI shows an enlarged rounded right level II node with necrotic foci (long arrow) and ill-defined margins (extracapsular spread). Short arrow shows the tongue primary reaching vallecula

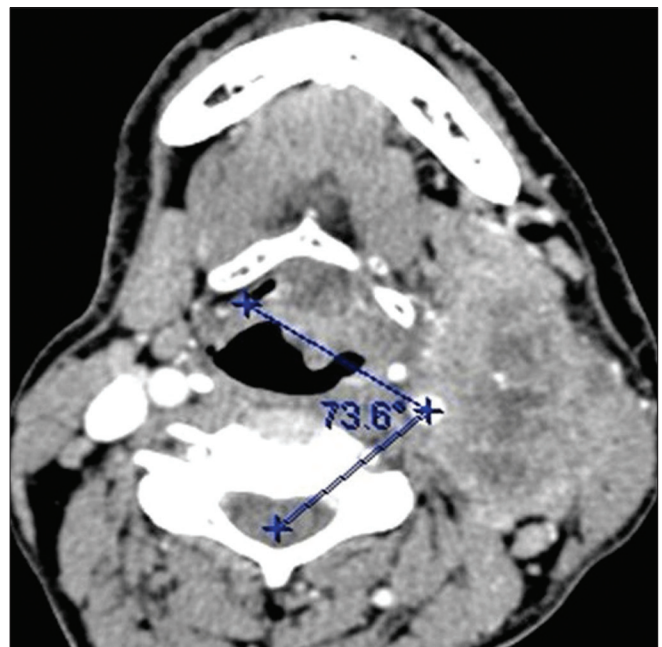
Figure 30: Large left level II node with necrosis and extracapsular spread (ill-defined margins and loss of planes with adjacent structures). Circumferential contact with common carotid artery measured on PACS is 360°-74°= 286° (unresectable)

Table 3: Tongue and Floor of mouth cancers

Imaging Modality- MRI with postgadolinium sequences and diffusion weighted imaging (one stop shop for primary and nodes)

Checklist

  Epicenter and tumor thickness.

  Involvement of extrinsic muscles and muscles of floor of mouth.

  Extent upto or across midline; involvement of ipsilateral and contralateral vascular bundle.

  Posterior extent to base tongue, tonsil and rest of oropharynx, preepiglottic space and hyoid bone.

  Posterior extent to masticator space and pterygoid plates

  Mandibular involvement and extent.

  Nodal status–number & size of abnormal nodes, level, presence of necrosis/extracapsular spread, invasion of adjacent structures and vessels

imaging modalities for detecting neck nodes and concludes that US-guided FNA is the most reliable technique to assess lymph node metastases in head and neck cancers.[54] Ultrasonography can be used to observe the N0 neck if the decision is not to perform elective neck dissection. The disadvantage of US and guided FNA, however, is the lack of widely available expertise. CT has a sensitivity varying from 55% to 95 % and a specificity of 39%-96% for assessing neck node metastases in various series while the reported sensitivity and specificity for MRI has been 64%-92% and 40%-81%.[54] Newer morphological criteria on T2W MR imaging for assessing neck nodes[55] and reports on diffusion weighted MRI[56,57] promise increased accuracy of MR imaging for detecting metastatic neck nodes [Figure 28].

CT or MRI ordered for the primary may detect metastatic nodes that may appear enlarged and rounded, show necrosis [Figure 29], extracapsular spread and invasion of adjacent structures. Necrosis is the most reliable criterion of metastasis. For non-necrotic homogenous nodes, various size criteria using maximum longitudinal diameter and minimum axial diameters have been specified, but false positive and false negative rates of 15-20 % are still seen as metastasis can occur in subcentimeter nodes.[58] The nodes in the draining region of the primary need close scrutiny. Bulky nodes at multiple levels and extranodal spread require postoperative irradiation. Circumferential contact of node with the carotid artery of more than 270 degrees precludes resectability of node and needs mention.[59] This measurement is ideally done using the angle measurement tool on the PACS/workstations. When the angle exceeds 180°, the tool automatically measures the smaller angle and the actual measurement is obtained by subtracting from 360° [Figure 30].

To summarize, imaging is essential in the management of oral cancers. It augments clinical findings to plan appropriate therapy. When surgery is contemplated, it provides information about resectability, extent of resection and reconstruction. Information from imaging can also indicate treatment outcomes.

References

1. Sankaranarayan R, Masuyer E, Swaminathan R, Ferley J, Whelan S. Head and neck cancer: A global perspective on epidemiology and prognosis. Anticancer Res 1998;18:4779-86.
2. Close L, Larson D, Shah JP. Essentials of Head and Neck Oncology. Stuttgart, Germany: Thieme Medical Publishers; 1998.
3. Som PM, Curtin HD. Head and Neck Imaging. 5th ed. Mosby: Elsevier; 2011. p. 1623-8.
4. Shah JP, Gil Z. Current concepts in management of oral cancer—surgery. Oral Oncol 2009;45:394-401.
5. NCCN Guidelines Version 1.2012, Cancer of the Oral Cavity, National Comprehensive Cancer Care Clinical Practice Guidelines in Oncology (NCCN Guidelines). NCCN.org.
6. Misra S, Chaturvedi A, Misra NC. Management of gingivobuccal complex cancer. Ann R Coll Surg Engl 2008;90:546-53.
7. Walvekar RR, Chaukar DA, Deshpande MS, Pai PS, Chaturvedi P, Kakade AC, et al. Prognostic factors for loco-regional failure in early stage (I and II) squamous cell carcinoma of the gingivobuccal complex. Eur Arch Otorhinolaryngol 2010;267:1135-40.
8. Walvekar RR, Chaukar DA, Deshpande MS, Pai PS, Chaturvedi P, Kakade A, et al. Squamous cell carcinoma of the gingivobuccal complex: Predictors of locoregional failure in stage III-IV cancers. Oral Oncol 2009;45:135-40.
9. Kimura Y, Sumi M, Sumi T, Ariji Y, Ariji E, Nakamura T. Deep extension from carcinoma arising from the gingiva: CT and MR imaging features. AJNR Am J Neuroradiol 2002;23:468-72.
10. Yen TC, Chang JT, Ng SH, Chang YC, Chan SC, Wang HM, et al. Staging of untreated squamous cell carcinoma of buccal mucosa with 18F-FDG PET: Comparison with head and neck CT/MRI and histopathology. J Nucl Med 2005;46:775-81.
11. Ng SH, Yen TC, Liao CT, Chang JT, Chan SC, Ko SF, et al. 18F-FDG PET and CT/MRI in oral cavity squamous cell carcinoma: A prospective study of 124 patients with histologic correlation. J Nucl Med 2005;46:1136-43.
12. Mukherji SK, Isaacs DL, Creager A, Shockley W, Weissler M, Armao D. CT detection of mandibular invasion by squamous cell carcinoma of the oral cavity. AJR Am J Roentgenol 2001;177:237-43.
13. Imaizumi A, Yoshino N, Yamada I, Nagumo K, Amagasa T, Omura K, et al. A potential pitfall of MR imaging for assessing mandibular invasion of squamous cell carcinoma in the oral cavity. AJNR Am J Neuroradiol 2006;27:114-22.
14. Seitz O, Chambron-Pinho N, Middendorp M, Sader R, Mack M, Vogl TJ, et al. 18F-Fluorodeoxyglucose-PET/CT to evaluate tumor, nodal disease, and gross tumor volume of oropharyngeal and oral cavity cancer: Comparison with MR imaging and validation with surgical specimen. Neuroradiology 2009;51:677-86.
15. Schöder H, Carlson DL, Kraus DH, Stambuk HE, Gönen M, Erdi YE, et al. 18F-FDG PET/CT for detecting nodal metastases in patients with oral cancer staged N0 by clinical examination and CT/MRI. J Nucl Med 2006;47:755-62.
16. Weissman JL, Carrau RL. "Puffed-cheek" CT improves evaluation of the oral cavity. AJNR Am J Neuroradiol 2001;22:741-4.
17. Henrot P, Blum A, Toussaint B, Troufleau P, Stines J, Roland J. Dynamic maneuvers in local staging of head and neck malignancies with current imaging techniques: Principles and clinical applications. Radiographics 2003;23:1201-13.
18. Spector ME, Gallagher KK, McHugh JB, Mukherji SK. Correlation

of radiographic and pathologic findings of dermal lymphatic invasion in head and neck squamous cell carcinoma. AJNR Am J Neuroradiol 2012;33:462-4.

19. Liao CT, Ng SH, Chang JT, Wang HM. T4b oral cavity cancer below the mandibular notch is resectable with a favorable outcome. Oral Oncol 2007;43:570-9.

20. Cummings C, Flint PW, Harker LA. Otolaryngology, Head and Neck surgery. 4th ed. Elsevier Mosby.

21. Standring S. Gray's Anatomy, The Anatomical Basis of Clinical Practice. 40th ed. Philadelphia: Churchill Livingstone Elsevier; 2011.

22. Ginsberg LE. Perineural tumor spread associated with head and neck malignancies. In: Som PM, Curtin HD, editors. Head and Neck Imaging. 5th ed. St Louis, Missouri, USA: Elsevier Mosby; 2011. p. 1021-39.

23. Pathak KA, Agarwal R, Deshpande MS. Marginal mandibulectomy for lateral sulcus tumours. Eur J Surg Oncol 2004;30:804-6.

24. Pathak KA, Shah BC. Marginal mandibulectomy: 11 years of institutional experience. J Oral Maxillofac Surg 2009;67:962-7.

25. Rao LP, Das SR, Mathews A, Naik BR, Chacko E, Pandey M. Mandibular invasion in oral squamous cell carcinoma: Investigation by clinical examination and orthopantomogram. Int J Oral Maxillofac Surg 2004;33:454-7.

26. Close LG, Burns DK, Merkel M, Schaefer SD. Computed tomography in the assessment of mandibular invasion by intraoral carcinoma. Ann Otol Rhinol Laryngol 1986;95:383-7.

27. Shaha AR. Preoperative evaluation of the mandible in patients with carcinoma of the floor of the mouth. Head Neck 1991;13:398-402.

28. Brown JS, Griffith JF, Phelps PD, Browne RM. A comparison of different imaging modalities and direct inspection after periosteal stripping in predicting the invasion of the mandible by oral squamous cell carcinoma. Br J Oral Maxillofac Surg 1994;32:347-59.

29. van den Brekel MW, Runne RW, Smeele LE, Tiwari RM, Snow GB, Castelijns JA, *et al*. Assessment of tumor invasion into the mandible: The value of different imaging techniques. Eur Radiol 1998;8:1552-7.

30. Lane AP, Buckmire RA, Mukherji SK, Pillsbury HC, Meredith SD. Use of computed tomography in the assessment of mandibular invasion in carcinoma of the retromolar trigone. Otolaryngol Head Neck Surg 2000;122:673-7.

31. Curran AJ, Toner M, Quinn A, Wilson G, Timon C. Mandibular invasion diagnosed by SPECT. Clin Otolaryngol 1996;21:542-5.

32. Weissman RA, Kimmelman CP. Bone scanning in the assessment of mandibular invasion by oral cavity carcinomas. Laryngoscope 1982;92:1-4.

33. Brockenbrough JM, Petruzzelli GJ, Lomasney L. Denta Scan as an accurate method of predicting mandibular invasion in patients with squamous cell carcinoma of the oral cavity. Arch Otolaryngol Head Neck Surg 2003;129:113-7.

34. Vidiri A, Guerrisi A, Pellini R, Manciocco V, Covello R, Mattioni O, *et al*. Multi-detector row computed tomography (MDCT) and magnetic resonance imaging (MRI) in the evaluation of the mandibular invasion by squamous cell carcinomas (SCC) of the oral cavity. Correlation with pathological data. J Exp Clin Cancer Res 2010;29:73.

35. Handschel J, Naujoks C, Depprich RA, Kübler NR, Kröpil P, Kuhlemann J, *et al*. CT- scan is a valuable tool to detect mandibular involvement in oral cancer patients. Oral Oncol 2012;48:361-6.

36. Elango JK, Gangadharan P, Sumithra S, Kuriakose MA. Trends of head and neck cancers in urban and rural India. Asian Pac J Cancer Prev 2006;7:108-12.

37. Dammann F, Horger M, Mueller-Berg M, Schlemmer H, Claussen CD, Hoffman J, *et al*. Rational diagnosis of squamous cell carcinoma of the head and neck region: Comparative evaluation of CT, MRI, and 18FDG PET. AJR Am J Roentgenol 2005;184:1326-31.

38. Lufkin RB, Wortham DG, Dietrich RB, Hoover LA, Larrsen SG, Kangarloo H, *et al*. Tongue and oropharynx: Findings on MR imaging. Radiology 1986;161:69-75.

39. Sigal R, Zagdanski AM, Schwaab G, Bosq J, Auperin A, Laplanche A, *et al*. CT and MR imaging of squamous cell carcinoma of tongue and floor of mouth. Radiographics 1996;16:787-810.

40. Yasumoto M, Shibuya H, Takeda M, Korenaga T. Squamous cell carcinoma of the oral cavity: MR findings and value of T1- versus T2-weighted fast spin-echo images. AJR Roentgenol 1995;164:981-7.

41. El-Naaj IA, Leiser Y, Shveis M, Sabo E, Peled M. Incidence of oral cancer occult metastasis and survival of T1-T2N0 oral cancer patients. J Oral Maxillofac Surg 2011;69:2674-9.

42. Huang SH, Hwang D, Lockwood G, Goldstein DP, O'Sullivan B. Predictive value of tumor thickness for cervical lymph-node involvement in squamous cell carcinoma of the oral cavity: A Meta-analysis of Reported Studies. Cancer 2009;115:1489-97.

43. Arakawa A, Tsuruta J, Nishimura R, Sakamoto Y, Korogi Y, Baba Y, *et al*. MR imaging of lingual carcinoma: Comparison with surgical staging. Radiat Med 1996;14:25-9.

44. Iwai H, Kyomoto R, Ha-Kawa SK, Lee S, Yamashita T. Magnetic resonance determination of tumor thickness as predictive factor of cervical metastasis in oral tongue carcinoma. Laryngoscope 2002;112:457-61.

45. Lam P, Au-Yeung KM, Cheng PW, Wei WI, Yuen AP, Trendell-Smith N, *et al*. Correlating MRI and histologic tumor thickness in the assessment of oral tongue cancer. AJR Am J Roentgenol 2004;182:803-8.

46. Preda L, Chiesa F, Calabrese L, Latronico A, Bruschini R, Leon ME, *et al*. Relationship between histologic thickness of tongue carcinoma and thickness estimated from preoperative MRI. Eur Radiol 2006;16:2242-8.

47. Okura M, Iida S, Aikawa T, Adachi T, Yoshimura N, Yamada T, *et al*. Tumor thickness and paralingual distance of coronal MR imaging predicts cervical node metastases in oral tongue carcinoma. AJNR Am J Neuroradiol 2008;29:45-50.

48. Kodama M, Khanal A, Habu M, Iwanaga K, Yoshioka I, Tanaka T, *et al*. Ultrasonography for intraoperative determination of tumor thickness and resection margin in tongue carcinomas. J Oral Maxillofac Surg 2010;68:1746-52.

49. Natori T, Koga M, Anegawa E, Nakashima Y, Tetsuka M, Yoh J, *et al*. Usefulness of intra-oral ultrasonography to predict neck metastasis in patients with tongue carcinoma. Oral Dis 2008;14:591-9.

50. Som PM. Detection of metastasis in cervical lymph nodes: CT and MR criteria and differential diagnosis. AJR Am J Roentgenol 1992;158:961-9.

51. Fasunla AJ, Greene BH, Timmesfeld N, Wiegand S, Werner JA, Sesterhenn AM. A meta-analysis of the randomized controlled trials on elective neck dissection versus therapeutic neck dissection in oral cavity cancers with clinically node-negative neck. Oral Oncol 2011;47:320-4.

52. D'Cruz AK, Dandekar MR. Elective versus therapeutic neck dissection in the clinically node negative neck in early oral cavity cancers: Do we have the answer yet? Oral Oncol 2011;47:780-2.

53. D'Cruz AK, Siddachari RC, Walvekar RR, Pantvaidya GH, Chaukar DA, Deshpande MS, *et al*. Elective neck dissection for the management of the N0 neck in early cancer of the oral tongue: Need for a randomized controlled trial. Head Neck 2009;31:618-24.

54. de Bondt RB, Nelemans PJ, Hofman PA, Casselman JW, Kremer B, van Engelshoven JM, *et al*. Detection of lymph node metastases in head and neck cancer: A meta-analysis comparing US, USgFNAC, CT and MR imaging. Eur J Radiol 2007;64:266-72.

55. de Bondt RB, Nelemans PJ, Bakers F, Casselman JW, Peutz-Kootstra C, Kremer B, *et al*. Morphological MRI criteria

improve the detection of lymph node metastases in head and neck squamous cell carcinoma: Multivariate logistic regression analysis of MRI features of cervical lymph nodes. Eur Radiol 2009;19:626-33.

56. Sumi M, Sakihama N, Sumi T, Morikawa M, Uetani M, Kabasawa H, *et al*. Discrimination of metastatic cervical lymph nodes with diffusion-weighted MR imaging in patients with head and neck cancer. AJNR Am J Neuroradiol 2003;24:1627-34.

57. Perrone A, Guerrisi P, Izzo L, D'Angeli I, Sassi S, Mele LL, *et al*. Diffusion-weighted MRI in cervical lymph nodes: Differentiation between benign and malignant lesions. Eur J Radiol 2011;77:281-6.

58. Som PM, Brandwein-Gensler MS. Lymph Nodes of the Neck. In: Som PM, Curtin HD, editors, Head and Neck Imaging. Vol 2. 5th ed. Philadelphia: Elsevier Mosby; 2011. p. 2287-383.

59. Yousem DM, Gad K, Tufano RP. Resectability issues with head and neck cancer. AJNR Am J Neuroradiol 2006;27:2024-36.

New features on the journal's website

Optimized content for mobile and hand-held devices

HTML pages have been optimized of mobile and other hand-held devices (such as iPad, Kindle, iPod) for faster browsing speed.
Click on **[Mobile Full text]** from Table of Contents page.
This is simple HTML version for faster download on mobiles (if viewed on desktop, it will be automatically redirected to full HTML version)

E-Pub for hand-held devices

EPUB is an open e-book standard recommended by The International Digital Publishing Forum which is designed for reflowable content i.e. the text display can be optimized for a particular display device.
Click on **[EPub]** from Table of Contents page.
There are various e-Pub readers such as for Windows: Digital Editions, OS X: Calibre/Bookworm, iPhone/iPod Touch/iPad: Stanza, and Linux: Calibre/Bookworm.

E-Book for desktop

One can also see the entire issue as printed here in a 'flip book' version on desktops.
Links are available from Current Issue as well as Archives pages.
Click on e View as eBook